PROCEEDINGS OF SCIENCE

High-E_{T} isolated-photon plus jets production in pp collisions at $\sqrt{s} = 8$ TeV with the ATLAS detector

Hector De La Torre on behalf of the ATLAS Collaboration
Michigan State University (US)
E-mail: hector.de.la.torre.perez@cern.ch

The dynamics of isolated-photon plus one-, two- and three-jet production in pp collisions at a centre-of-mass energy of 8 TeV are studied with the ATLAS detector at the LHC using a data set with an integrated luminosity of 20.2 fb^{-1}. Measurements of isolated-photon plus jets cross sections are presented as functions of the photon and jet transverse momenta. The cross sections as functions of the azimuthal angle between the photon and the jets, the azimuthal angle between the jets, the photon–jet invariant mass and the scattering angle in the photon–jet centre-of-mass system are presented. The pattern of QCD radiation around the photon and the leading jet is investigated by measuring jet production in an annular region centred on each object; enhancements are observed around the leading jet with respect to the photon in the directions towards the beams. The experimental measurements are compared to several different theoretical calculations, and overall a good description of the data is found.

ATL-PHYS-PROC-2017-068
20 June 2017

25th International Workshop on Deep Inelastic Scattering and Related Topics
3-7 April 2017
University of Birmingham, Birmingham, UK

1. Introduction

These proceedings include a review of the measurement of cross sections for isolated-photon plus one-, two- and three-jet final states as functions of several variables related to the kinematics, dynamics and scale evolution of the process performed with the ATLAS detector [1] at the Large Hadron Collider (LHC) [2] at a centre-of-mass energy of $\sqrt{8}$ TeV . In addition, the jet production around the leading jet and photon is studied in photon plus two jets events using variables sensitive to the pattern of parton radiation around both objects [3].

The production of prompt photons in association with jets in proton–proton collisions, $pp \to \gamma + \text{jets} + \text{X}$, provides a testing ground for perturbative QCD (pQCD) with a hard colourless probe less affected by hadronisation effects than jet production. The measurements of the angular correlations between the photon and the jets can be used to probe the dynamics of the hard-scattering process. Since the dominant production mechanism in pp collisions at the LHC proceeds via the $qg \to q\gamma$ process, measurements of prompt-photon plus jet production are useful in constraining the gluon density in the proton. These measurements can also be used to tune the Monte Carlo (MC) models and to test t-channel quark exchange [4].

In this review, the next-to-leading-order (NLO) QCD predictions from JETPHOX [5] are compared with the photon plus one-jet measurements, whereas those from BLACKHAT [6] are compared with the photon plus two-jet and photon plus three-jet measurements. In addition, the predictions from event generators PYTHIA [7] and SHERPA [8] are also compared with the measurements.

2. Data selection

The data used in this analysis were collected during the proton–proton collision running period of 2012, when the LHC operated at a centre-of-mass energy of $\sqrt{s} = 8$ TeV. Only events taken in stable beam conditions and passing detector and data-quality requirements are considered. Events were recorded using a single-photon trigger, with a nominal transverse energy threshold of 120 GeV; this trigger is used offline to select events in which the photon transverse energy, after reconstruction and calibration, is greater than 130 GeV. The integrated luminosity of the collected sample is 20.2 ± 0.4 fb^{-1} [9].

2.1 Object selection

The selection of photon candidates is based on energy clusters reconstructed in the electromagnetic calorimeter with transverse energies exceeding 2.5 GeV. The clusters are matched to charged-particle tracks to differentiate between electrons and photons [10].

Events with at least one photon candidate with calibrated $E_{\text{T}}^{\gamma} > 130$ GeV and $|\eta^{\gamma}| < 2.37$ are selected; Shower-shape identification requirements are applied to the candidates to remove non-prompt photons from hadron decays are applied to the candidates;

The photon candidate is required to be isolated based on the amount of transverse energy in a cone of size $\Delta R = 0.4$ around the photon. The isolation transverse energy is computed from three-dimensional topological clusters of calorimeter cells (topo-clusters) and is denoted by $E_{\text{T,det}}^{\text{iso}}$. The energy of the photon itself is subtracted from the calculation. After leakage and pileup corrections

$E_{\mathrm{T,det}}^{\mathrm{iso}}$ is required to be lower than 4.8 GeV $+ 4.2 \cdot 10^{-3} \cdot E_{\mathrm{T}}^{\gamma}$ [GeV]. This isolation requirement is necessary to avoid the large contribution from neutral-hadrons decaying into photons.

Jets are reconstructed using the anti-k_t algorithm with radius parameter $R = 0.6$ [11]. The inputs to the jet reconstruction are topo-clusters.

Good quality jets are required to have calibrated transverse momenta greater than 50 GeV and rapidity $|y^{\mathrm{jet}}| < 4.4$.

2.2 Event categorisation

To investigate the production of jets in association with a photon, three main samples are selected according to the leading (jet1), sub-leading (jet2), and sub-sub-leading (jet3) jets p_{T} values. To study photon plus one-jet events $p_{\mathrm{T}}^{\mathrm{jet1}} > 100$ GeVis required, to study photon plus two-jet events $p_{\mathrm{T}}^{\mathrm{jet1}} > 100$ GeV and $p_{\mathrm{T}}^{\mathrm{jet2}} > 65$ GeVare required and to study photon plus three-jet events $p_{\mathrm{T}}^{\mathrm{jet1}} > 100$ GeV, $p_{\mathrm{T}}^{\mathrm{jet2}} > 65$ GeV and $p_{\mathrm{T}}^{\mathrm{jet3}} > 50$ GeVare required. The three samples are sequential subsets of each other.

To study the pattern of QCD radiation around the photon and jet1, two additional samples of photon plus two-jet events are selected. The phase-space regions are defined to avoid biases due to different p_{T} and η requirements on the final-state objects as well as to have no overlap between the two samples. Both samples must satisfy $p_{\mathrm{T}}^{\mathrm{jet1}} > 130$ GeV, $|\eta^{\mathrm{jet1}}| < 2.37$ and $p_{\mathrm{T}}^{\mathrm{jet2}} > 50$ GeV, and the angular distance between the photon and jet1, $\Delta R^{\gamma-\mathrm{jet1}}$, is restricted to $\Delta R^{\gamma-\mathrm{jet1}} > 3$

The cross sections are measured as functions of β^{γ} and β^{jet1} which are defined as:

$$\beta^{x} = \tan^{-1} \frac{|\phi^{\mathrm{jet2}} - \phi^{x}|}{\mathrm{sign}(\eta^{x}) \cdot (\eta^{\mathrm{jet2}} - \eta^{x})}, \tag{2.1}$$

where x may be γ or jet1 and represent the angle in the η–ϕ plane of jet2 around the photon or jet1 respectively, defined in such a way that $\beta^{x} = 0$ (π) always points to the beam which is closer to (farther from) the photon or jet1 in the η–ϕ plane.

To measure β^{γ} the phase space is restricted to $1 < \Delta R^{\gamma-\mathrm{jet2}} < 1.5$. In addition, $p_{\mathrm{T}}^{\mathrm{jet2}} < E_{\mathrm{T}}^{\gamma}$ is imposed for comparison with the other sample while to measure β^{jet1}, the phase-space is restricted to $1 < \Delta R^{\mathrm{jet1}-\mathrm{jet2}} < 1.5$

Schematic diagrams for the definitions of β^{γ} and β^{jet1} are shown in Figure 1.

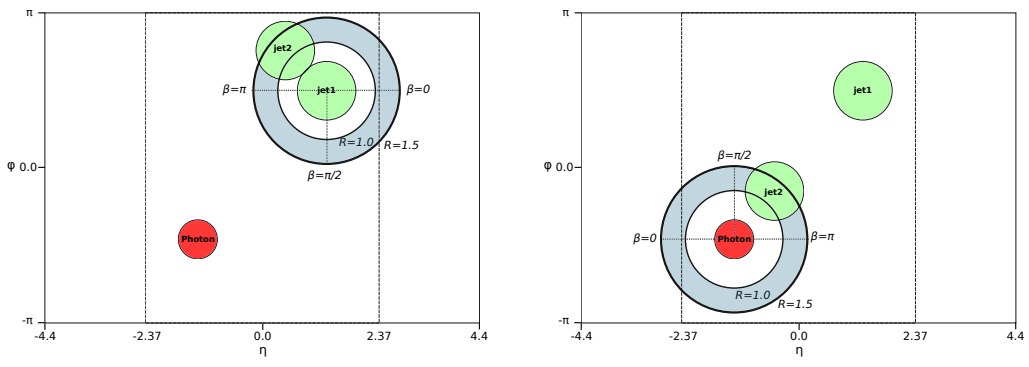

Figure 1: Schematic diagrams that show the definitions of (a) β^{γ} and (b) β^{jet1} [3].

3. Signal extraction and cross-section measurement

A non-negligible background contribution from jets remains in the selected sample, even after identification and isolation requirements on the photon. The background subtraction uses a data-driven method based on signal-suppressed control regions. The background contamination is estimated using a two-dimensional sideband technique and then subtracted bin-by-bin from the observed yield. Four regions are defined using the two-dimensional plane formed by $E_{\mathrm{T}}^{\mathrm{iso}}$ and the photon identification variable: The signal region that contains well identified ("tight") photons and all of the remaining combinations of tight, non-tight, isolated and non-isolated photons.

The cross sections are corrected to the particle level using the bin-by-bin method that uses the formula

$$\frac{\mathrm{d}\sigma}{\mathrm{d}A}(i) = \frac{N_A^{\mathrm{sig}}(i)\, C^{\mathrm{MC}}(i)}{\mathscr{L}\, \Delta A(i)}, \tag{3.1}$$

where the bin-by-bin corrections factors $C^{\mathrm{MC}}(i)$ are obtained using SHERPA MC signal samples.

4. Results

The cross section for photon plus one-jet is measured as a function of $|\cos\theta^*|$ for 467 GeV $> m^{\gamma-\mathrm{jet1}} >$ 2.45 TeV as shown in Figure 2(a). For this measurement additional constraints are needed to remove biases due to the rapidity and transverse momentum requirements on the photon and jet1 [4] and are indicated in the legend. The NLO QCD predictions from JETPHOX give a good description in both shape and normalisation.

Photon plus two-jet production is investigated by measuring the cross section as a function of E_{T}^{γ} for $p_{\mathrm{T}}^{\mathrm{jet1}} > 100$ GeV and $p_{\mathrm{T}}^{\mathrm{jet2}} > 65$ GeV and is shown in Figure 2(b). The NLO QCD predictions from BLACKHAT provide a good description of the measurements for $E_{\mathrm{T}}^{\gamma} < 750$ GeV.

Photon plus three-jet production is characterised by measurements of cross sections as functions of $p_{\mathrm{T}}^{\mathrm{jet3}}$ and the angular correlation between the photon and jet3 for $p_{\mathrm{T}}^{\mathrm{jet1}} > 100$ GeV, $p_{\mathrm{T}}^{\mathrm{jet2}} >$ 65 GeV, and $p_{\mathrm{T}}^{\mathrm{jet3}} > 50$ GeV. They are shown in Figure 2(c) and 2(d) respectively. The NLO QCD predictions from BLACKHAT provide an adequate description of the measurements.

To compare the jet production around the photon and jet1, the cross sections for photon plus two-jet production as functions of β^{jet1} and β^{γ} are measured and shown in Figure 3. The predictions from SHERPA give a good description of the measured cross sections. To quantify the differences between the two measurements, the ratio of $\mathrm{d}\sigma/\mathrm{d}\beta^{\mathrm{jet1}}$ and $\mathrm{d}\sigma/\mathrm{d}\beta^{\gamma}$ is made. This ratio, shown in Figure 3(b), is enhanced at $\beta = 0$ and π rad with respect to the value of the ratio at $\beta = \pi/2$ rad which indicates that the pattern of QCD radiation around the photon and jet1 are different. The measured ratio is tested against the hypothesis of being independent of β and the resulting p-value is 1.3% [3].

5. Conclusion

Measurements of the cross sections for the production of an isolated photon in association with one, two or three jets in proton–proton collisions at $\sqrt{s} = 8$ TeV, using a data set with an integrated

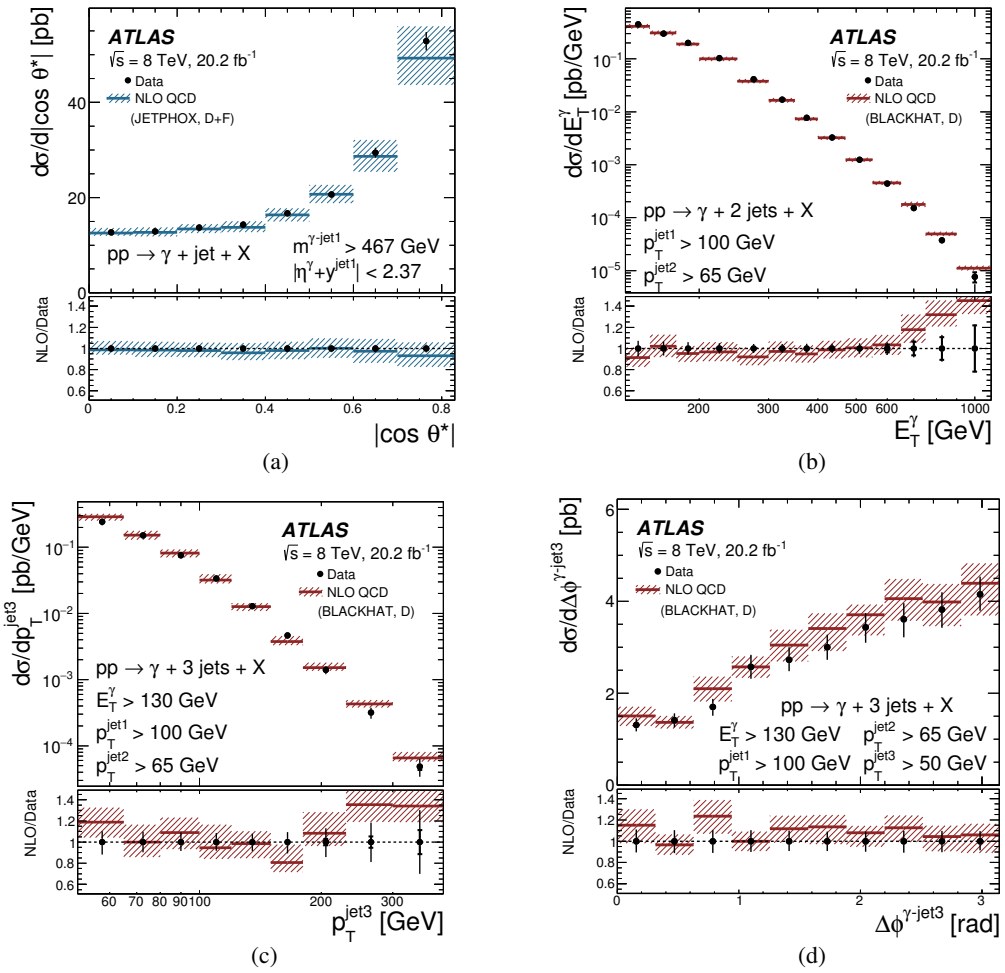

Figure 2: Measured cross section for (a) isolated-photon plus one-jet production (dots) as a function of $|\cos\theta^*|$, (b) for isolated photon plus two-jet production as a function of E_{T}^{γ} and (c) for isolated photon plus three-jet production as a function of $p_{\mathrm{T}}^{\mathrm{jet3}}$ and (d) $\Delta\phi^{\gamma-\mathrm{jet3}}$. The NLO QCD predictions from JETPHOX in (a) and BLACKHAT in (b), (c) and (d) corrected for hadronisation and underlying-event effects are also shown . The inner (outer) error bars represent the statistical uncertainties (the statistical and systematic uncertainties added in quadrature) and the shaded band represents the theoretical uncertainty [3].

luminosity of 20.2 fb^{-1} recorded by the ATLAS detector at the LHC are presented. They provide stringent tests of pQCD and scrutinise the description of the dynamics of isolated-photon plus jets production in pp collisions. The full collection of measurements as functions of fifteen different variables may be found in [3].

The patterns of QCD radiation around the photon and the leading jet are compared by measuring the production of the subleading jet in an annular region centred on the given final-state object. The cross sections as functions of β^{γ} and β^{jet1} are observed to be different. The ratio of the cross sections shows enhancements in the directions towards the beams, $\beta = 0$ and π rad.

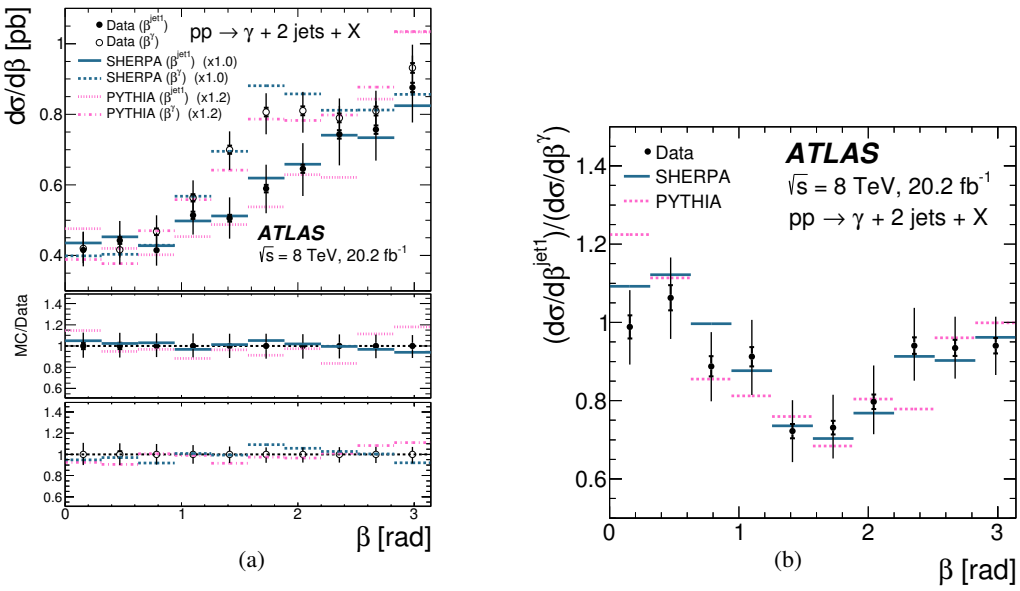

Figure 3: (a) Measured cross sections for isolated-photon plus two-jet production as functions of β^{jet1} (dots) and β^{γ} (open circles). For comparison, the predictions from SHERPA (blue solid and dashed lines) and PYTHIA (pink dash-dotted and dotted lines) normalised to the integrated measured cross sections (using the factors indicated in parentheses) are also shown. (b) Ratio of the measured cross-section $\mathrm{d}\sigma/\mathrm{d}\beta^{\text{jet1}}$ and $\mathrm{d}\sigma/\mathrm{d}\beta^{\gamma}$ (dots); the ratios for the SHERPA and PYTHIA predictions are shown as solid and dashed lines, respectively. The inner (outer) error bars represent the statistical uncertainties (the statistical and systematic uncertainties added in quadrature) [3].

References

[1] ATLAS Collaboration, JINST **3** (2008) S08003.

[2] L.Evans and P.Briant (editors), JINST **3** (2008) S08001.

[3] ATLAS Collaboration, Nucl. Phys. B **918** (2017) 257, arXiv:1611.06586 [hep-ex].

[4] ATLAS Collaboration, Nucl. Phys. B **875** (2013) 483, arXiv:1307.6795 [hep-ex].

[5] S. Catani, M. Fontannaz, J. Ph. Guillet and E. Pilon, JHEP **05** (2002) 028, arXiv:hep-ph/0204023 [hep-ph].

[6] C.F. Berger et al., Phys. Rev. D **78** (2008) 036003, arXiv:0803.4180 [hep-ph].

[7] T. Sjöstrand, S. Mrenna and P.Z. Skands, Comput. Phys. Commun. **178** (2008) 852, arXiv:0710.3820 [hep-ph].

[8] T. Gleisberg et al., JHEP **02** (2009) 007, arXiv:0811.4622 [hep-ph].

[9] ATLAS Collaboration, ATLAS Collaboration, Eur. Phys. J. C **76** (2016) 653, arXiv:1608.03953 [hep-ex].

[10] ATLAS Collaboration, M. Aaboud et al., Eur. Phys. J. C **76** (2016) 666, arXiv:1606.01813 [hep-ex].

[11] M. Cacciari, G. Salam and G. Soyez, JHEP **04** (2008) 063, arXiv:0802.1189 [hep-ph].